Global hotspots of recent and ancestral turnover in birds

Ian R. McFadden[1,2*], Marco Túlio P. Coelho[3], Rafael O. Wüest[1], Fernanda A. S. Cassemiro[3], Niklaus E. Zimmermann[1], Loïc Pellissier[1,2], Thiago F. Rangel[3], Catherine H. Graham[1]

[1]Swiss Federal Institute for Forest, Snow and Landscape Research (WSL), Zürcherstrasse 111, 8903 Birmensdorf, Switzerland

[2]Institute of Terrestrial Ecosystems, Department of Environmental Systems Science, ETH Zürich (Swiss Federal Institute of Technology), 8092, Zurich, Switzerland

[3]Department of Ecology, Institute of Biological Sciences, Federal University of Goiás, CP 131, 74.001-970 Goiânia, Goiás, Brazil

A primary goal of biodiversity research is to uncover the processes acting in space and time to create the global distribution of species richness. However, we currently lack an understanding of how recent versus ancient biodiversity dynamics shape patterns of diversity for most groups. Here, we introduce a method to partition lineage turnover into recent and ancestral components, and use it to identify hotspots of turnover at the global scale for 8,296 bird species. Counter to the tropical niche conservatism hypothesis, we find extra-tropical regions such as Greenland and the Sahara are hotspots of ancestral turnover, while areas with high climatic variation such as (sub)tropical mountains and biome transitions are recent turnover hotspots. We can now quantify the relative contribution of contemporary and ancient lineage dynamics to assemblage structure, which

enables future research to explore the processes generating earth's diversity in a more temporally-explicit framework.

The global distribution of species richness, abundance and traits is increasingly well-known for many groups[1–4], but the mapping of processes driving these patterns at large scales is in its infancy[5]. Uncovering the spatial structure of processes such as speciation, extinction and dispersal can help solve debates about how lineage dynamics at different timescales create observed patterns[6,7], and how these processes vary across the surface of the earth[5,8]. In addition, such information could be used to inform conservation efforts that work to safeguard the creation of future biodiversity by preserving key areas where biodiversity generation is ongoing, or where unique lineages exist[9,10]. However, it has historically been difficult to determine the influence of past versus recent events on the structure of regional biotas and local assemblages[11,12], leading to several ongoing debates, for example about the formation of hyper-diverse regions such as the Andes and the Amazon[13].

Disentangling the influence of recent versus past events is crucial because it is increasingly understood that current diversity patterns are the result of processes acting at both recent and ancient time periods[14]. This is reflected in the museum versus cradle debate about the role of reduced extinction rates versus increased speciation rates as the primary source of regional diversity, and debates about the role of tectonic uplift and biome transitions as generators of environmental heterogeneity and diversity gradients[3,7,8,12,15,16]. Despite the need for a more temporally explicit view, many studies addressing these debates have relied on species-based

approaches which ignore evolutionary history, or examine biodiversity patterns in aggregate as opposed to focusing on the role of specific time periods.

One potentially powerful way to infer the processes shaping diversity is to quantify the spatial turnover of relatedness among assemblages across locations[17,18]. High levels of recent speciation, either locally or in lineages that disperse to an assemblage, or large differences between assemblages in present day climate, should tend to increase phylogenetic turnover in more recent lineages. In contrast, ancient speciation events, vicariance, and deep-time climatic changes should tend to increase the turnover of older lineages among sites[19]. However, existing phylogenetic turnover approaches average across many different time periods, possibly obscuring the effect of processes acting in different eras. In addition, existing metrics are sensitive to either recent or deep divergences, but not both, and studies employing these approaches are often limited in geographical and taxonomic scope[12,19,20].

Partitioning lineage turnover

To gain new insights into biodiversity dynamics across evolutionary time scales, we introduce a method to partition the spatial turnover of assemblages into two additive components, which represent recent versus ancient assemblage change (Fig. 1). This approach can therefore be used to identify specific regions where more modern versus deep-time dynamics may be structuring diversity most strongly. We use this method to identify global hotspots of lineage turnover for both recent and ancestral components by mapping mean turnover between neighboring 1-degree cells, using birds (class *Aves*) as a focal clade. We then ask how patterns of recent and ancestral turnover and the hotspots we identify are shaped by climate, earth surface topography and the evolutionary structure of assemblages. We predict that areas of recent turnover will be found in

tectonically active regions such as uplifting mountain ranges[3,15], and that ancestral turnover will be strongest in the tropics, because many lineages originated in and subsequently dispersed from these regions[16,21]. Finally, as a global test of the biome conservatism hypothesis[22], we predict that transitions between biomes and zoogeographic realms (*sensu* Holt et al. 2013) will favor elevated turnover of both partitions.

Our method to partition turnover along the phylogenetic scale consists of three main steps (Fig. 1, see 'Methods'). First, given a phylogeny encompassing two assemblages being compared, a threshold is chosen that represents the phylogenetic depth separating older from more recent portions of the tree. The recent segment is then created by collapsing to zero branch lengths older than the threshold, i.e. closer to the root of the phylogeny (Fig. 1B), and the ancestral segment is created by collapsing to zero branch lengths younger than the threshold, i.e. closer to the tips (Fig. 1C). Finally, recent ($p\beta_{Recent}$) and ancestral ($p\beta_{Ancestral}$) phylogenetic turnover fractions are calculated as the non-shared branch length in either the recent or ancestral segments (red and blue-colored branches in Fig. 1B, 1C), divided by the total branch length connecting both assemblages. Larger fractions indicate higher lineage turnover between two assemblages and smaller fractions signify lower turnover. Using this method, we can now determine if turnover is due to losses or gains of recently-diverged or deeper-diverging clades, and the relative influence of each. When mapping turnover, we used the recent and ancestral fractions that then sum to the total turnover at a given location, which may be higher or lower depending on the region.

Using a comprehensive phylogeny of all birds (see 'Methods'), we evaluated a series of thresholds to demarcate recent from ancestral turnover. We found results were largely the same

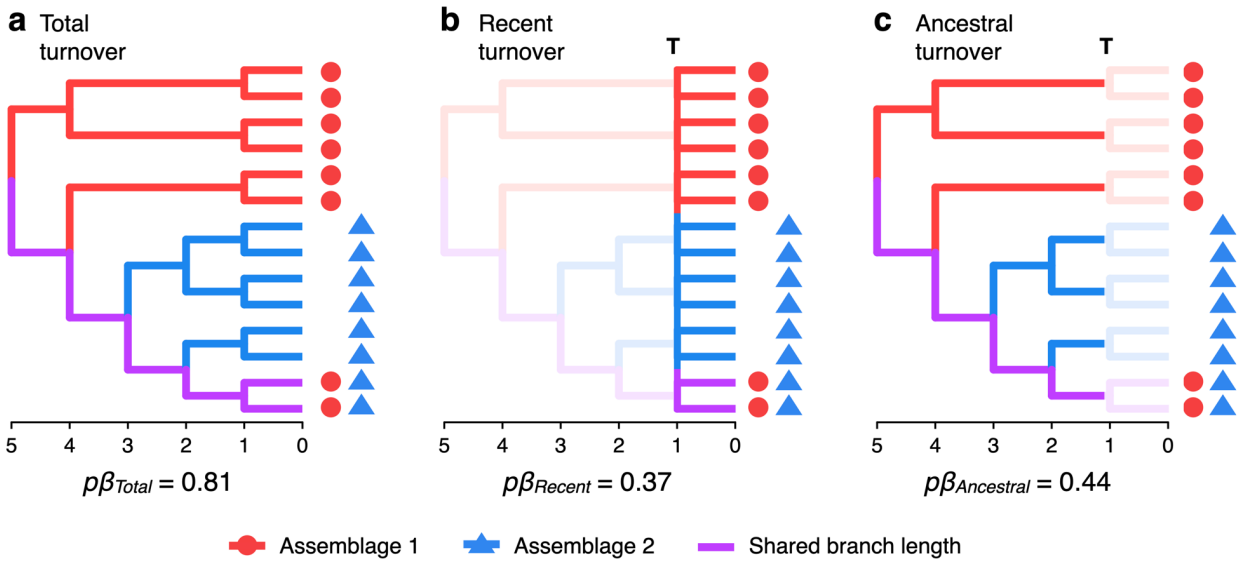

Figure 1 | Partitioning lineage turnover into recent and ancestral components. Visualization of total, recent and ancestral phylogenetic turnover, calculated as the fraction of total branch length (all colors) found only in a single assemblage (either red or blue branches) for the entire phylogeny (**a**) and more recent (**b**) versus more ancient (**c**) parts of a shared phylogeny (see 'Methods'). Assemblage membership is denoted with red circles or blue triangles and the phylogeny links all species in both assemblages. The location of the partition threshold used in this example, at a depth of 1myr, is denoted with *T*.

when an intermediate value was chosen (5myr), versus when older (10myr) or more recent (0.5myr) thresholds were used (Extended Data Fig. 1 and see 'Methods'). Therefore, we chose to use 5myr as a threshold, which also corresponds to the period of highest diversification in this group[24]. However, the most appropriate threshold will depend on the groups under study, and could also be chosen to correspond to geological or biological events thought to strongly influence diversity (e.g. Bacon et al. 2015). We measure phylogenetic turnover via the UniFrac metric[18], the phylogenetic analog of Jaccard dissimilarity. However, our method can be applied to any turnover metric that relies on branch lengths. We focus here on birds because they are ecologically important and intensely-studied, and thus taxonomic, distribution and phylogenetic information is essentially complete for all known species[24]. Finally, we quantified the effect of

environmental heterogeneity and topographic complexity on recent and ancestral turnover using global-scale climatic and topographic data (see 'Methods').

Results and discussion

Using our partitioning method, we discovered global hotspots of recent and ancestral turnover that occur in largely non-overlapping geographic and environmental space (Fig. 2). Surprisingly, the Sahara, Middle East and Greenland are all hotspots of ancestral turnover, while in contrast mountainous regions such as the Andes, East Africa and the Himalayas are hotspots of recent turnover (Fig. 2A, Extended Data Fig. 3). Our results clarify earlier work which identified similar regions of high turnover in birds[26,27] by uncovering the phylogenetic scales that most strongly structure this turnover. One explanation for these results is a large-scale geographic gradient in speciation, because variation in this process should leave imprints in the phylogenetic structure of assemblages[5,28]. Despite much spatial variation, the ancestral turnover fraction is on average higher than the fraction of recent turnover (Extended Data Fig. 3, $p\beta_{Ancestral}$: mean=0.11, s.d.=0.09, range=0-0.79; $p\beta_{Recent}$: mean=0.03, s.d.=0.02, range=0-0.16). In addition, several regions are hotspots of both forms of turnover. The existence of 'double hotspots' in tropical and subtropical mountain ranges such as the Andes and Himalayas, suggests species rich regions achieve their exceptional diversity by being both museums and cradles of diversity[3,29,30].

Counter to hypotheses of tropical niche conservatism and the 'tropics as museum'[31], ancestral turnover hotspots are not primarily located in the tropics, but are in climatically-extreme, species-poor regions such as North African and Middle East deserts, and Greenland (Fig. 2,

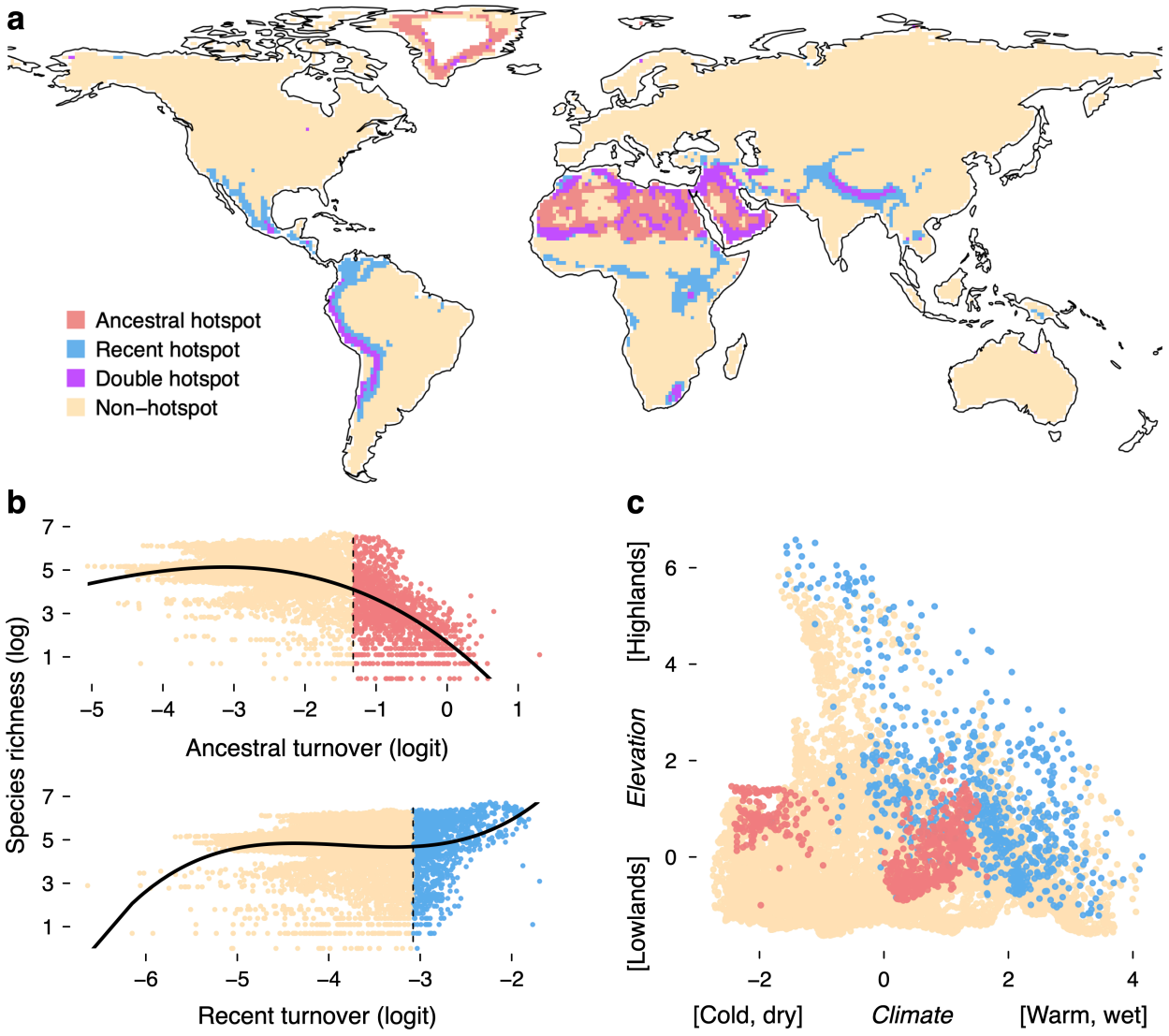

Figure 2 | Global distribution of turnover hotspots. (**a**) Geographic distribution of ancestral and recent turnover hotspots. Hotspots of both forms of turnover are shown in purple and all other areas (non-hotspots) are in tan. (**b**) Richness as a function of ancestral and recent turnover, fit via third degree polynomials due to non-linearity of the response. Points with x-axis values within hotspots are colored according to the corresponding hotspot type. (**c**) Distribution of recent and ancestral turnover hotspots in climatic and topographic space. See Extended Data Fig. 2 for PC axis loadings, and Extended Data Fig. 3 for continuous maps of the turnover partitions.

Extended Data Fig. 4). However, these patterns could potentially arise via tropical niche conservatism, if high ancestral turnover is shaped by independent colonizations of species

tolerant of extreme climates from disparate branches of the phylogeny. Another, non-mutually exclusive explanation is that turnover in species-poor regions is high because small numbers of species differing among localities creates large proportional turnover[26]. Indeed, we find tree topology, a metric incorporating species richness, phylogenetic diversity and tree depth, is a better predictor of ancestral turnover than either climate or topography (Fig. 3A, see 'Methods'). This richness effect may also partly explain why Greenland is a hotspot of ancestral turnover (Extended Data Fig. 5, Gaston et al. 2007, Barnagaud et al. 2017). Future, targeted work in specific regions could clarify the roles of niche conservatism and colonizations on species turnover and richness.

We find that climate and earth surface topography both influence turnover, but the relative importance of each differs between recent and ancestral partitions (Fig. 2C, Fig. 3). For example, ancestral hotspots occur in climatically-extreme environments, occupy a smaller fraction of topo-climatic space compared to recent turnover hotspots, and are found in two distinct areas of this space (Fig. 2C). This suggests that unproductive regions such as deserts and the Arctic can be hotspots of lineage turnover, unlike biodiversity hotspots (*sensu* Myers et al. 2000) which are primarily in highly-productive, tropical regions. In contrast to ancestral hotspots, hotspots of recent turnover are primarily distributed across tectonically-active regions such as the mountain chains of the Andes, East Africa and the Himalayas (Fig. 2A). Recent turnover hotspots also span a much larger area of topo-climatic space than ancestral hotspots, and are generally found on the margins of this space, in particular wet, warm, high elevation regions such as tropical mountains (Fig. 2C). Our findings contribute to an emerging consensus about the role of climatic heterogeneity, in particular across elevation, in generating global diversity patterns[2,3,34].

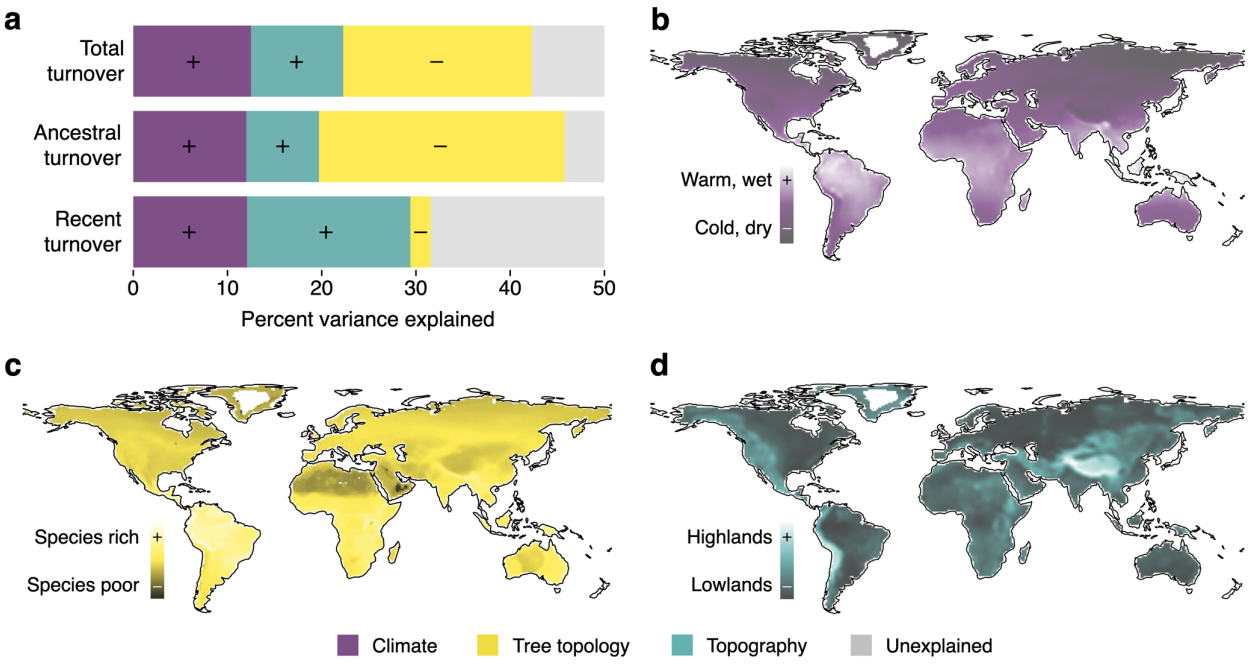

Figure 3 | Physical and biotic drivers of turnover. (**a**) Relative importance of physical and biotic factors for predicting total, ancestral and recent turnover; +/− indicates direction of effects. Principal component (PC) axes used in the analysis are plotted in geographic space for each assemblage: (**b**) climate, (**c**) tree topology, integrating species richness, phylogenetic diversity and tree depth (see 'Methods'), and (**d**) land surface topography (Extended Data Fig. 2).

Our hotspot map reveals that transitions between biomes and zoogeographic realms are often areas of high phylogenetic turnover, particularly of recent lineages. For example, several major turnover hotspots are in transition zones between grasslands and deserts in North Africa, plains and mountains in South Asia, and along the Isthmus of Panama separating North and South America (Fig. 2A). This serves as an independent test of the biome conservatism hypothesis, which posits that broad evolutionary conservatism acts at the broad climatic scale of biomes to structure assemblages[7,35]. Our results call for additional studies into the role of transitions between biomes and zoogeographic realms in generating the spatial distribution of diversity[9,22,30], especially as biomes are shifting due to anthropogenic impacts[36].

159

160 Emerging evidence suggests that large-scale gradients in species richness may be influenced by
161 gradients in species turnover, yet large-scale tests are few and results can differ based on the
162 choice of metric[30,37,38]. Here, we find areas of high avian richness are associated most often with
163 hotspots of recent turnover (Fig. 2A&B, Extended Data Fig. 4) and are found in biodiversity
164 hotspots (*sensu* Myers et al. 2000). This suggests that high species turnover, in particular of more
165 recent clades, contributes to richness gradients at large scales. However, the global relationship
166 between species richness and recent turnover is weak (R^2=0.02, df=12,495, $P < 2.2x10^{16}$), though
167 ancestral turnover is more predictive of richness (R^2=0.38, df=12,495, $P < 2.2x10^{16}$). As
168 mentioned previously, some regions of high ancestral turnover such as the Sahara and Greenland
169 are also hotspots of recent turnover. This suggests a possible role for high recent speciation rates
170 in these areas[28], though other factors such as immigration are likely important.
171
172 Though we found several new global diversity patterns, care needs to be taken when interpreting
173 results- for example some turnover metrics may be influenced by local or regional richness[38]. To
174 test for an influence of richness on our results, we compared geographic patterns in residuals of
175 regressions of both ancestral and recent turnover against richness (see 'Methods'). Counter to
176 expectations if local richness was largely shaping our results, we find strong patterns in the
177 residuals- for example many of the same areas identified as hotspots also had greater than
178 expected turnover given their richness (Extended Data Fig. 6). In addition, we removed the
179 bottom 10^{th}, 25^{th} and 50^{th} percentile of assemblages by richness and recalculated turnover
180 hotspots using the remaining regions (see 'Methods'). We find the Greenland hotspot is largely
181 removed without areas in the poorest 10th percentile, and the Sahara and Middle East hotspots

are partially removed after areas in the bottom 25th percentile are removed (Extended Data Fig. 7). Taken together, it appears the patterns of turnover identified here are not strongly influenced by local richness, but that, as noted earlier, hotspots of ancestral turnover are often in species-poor regions of the globe.

Combined, our results suggest that diversity in many regions of the globe is influenced more by recent than ancient dynamics, though both appear to be important for exceptional, hyper-diverse regions such as the Andes and the Himalayas[3]. Therefore, a steep reduction in human impacts in these areas is needed to maintain processes generating biodiversity now and into the future[9]. In addition, our results argue for the conservation of high turnover, low diversity hotspots such as the Sahara and Greenland, which are not currently classified as biodiversity hotspots but may be particularly sensitive to global change[36]. Using our approach, we provide both a global map of the recent and ancestral lineage structure of avian assemblages, and a foundation for further examination into the processes structuring species diversity in space and time.

1. Crowther, T. W. *et al.* Mapping tree density at a global scale. *Nature* **525**, 201–205 (2015).

2. Quintero, I. & Jetz, W. Global elevational diversity and diversification of birds. *Nature* **555**, 246–250 (2018).

3. Rahbek, C. *et al.* Humboldt's enigma: What causes global patterns of mountain biodiversity? *Science.* **365**, 1108–1113 (2019).

4. Diaz, S. *et al.* The global spectrum of plant form and function. *Nature* **529**, 167–171 (2016).

5. Rabosky, D. L. *et al.* An inverse latitudinal gradient in speciation rate for marine fishes. *Nature* **559**, 392–395 (2018).

6. Pontarp, M. *et al.* The latitudinal diversity gradient: novel understanding through mechanistic eco-evolutionary models. *Trends Ecol. Evol.* **34**, 211–223 (2019).

7. Ackerly, D. D. Adaptation, niche conservatism, and convergence: comparative studies of leaf evolution in the California chaparral. *Am. Nat.* **163**, 654–671 (2004).

8. Rangel, T. F. *et al.* Modeling the ecology and evolution of biodiversity: Biogeographical cradles, museums, and graves. *Science.* **361**, eaar5452 (2018).

9. Smith, T. B., Kark, S., Schneider, C. J., Wayne, R. K. & Moritz, C. Biodiversity hotspots and beyond: the need for preserving environmental transitions. *Trends Ecol. Evol.* **16**, 431 (2001).

10. Safi, K., Armour-Marshall, K., Baillie, J. E. M. & Isaac, N. J. B. Global patterns of evolutionary distinct and globally endangered amphibians and mammals. *PLoS One* **8**, e63582 (2013).

11. Ricklefs, R. E. Community diversity: relative roles of local and regional processes. *Science.* **235**, 167–171 (1987).

12. Mazel, F. *et al.* Global patterns of β-diversity along the phylogenetic time-scale: The role of climate and plate tectonics. *Glob. Ecol. Biogeogr.* **26**, 1211–1221 (2017).

13. Hoorn, C. *et al.* Amazonia through time: Andean uplift, climate change, landscape evolution, and biodiversity. *Science.* **330**, 927–931 (2010).

14. Graham, C. H., Storch, D. & Machac, A. Phylogenetic scale in ecology and evolution. *Glob. Ecol. Biogeogr.* **27**, 175–187 (2018).

15. Antonelli, A. *et al.* Geological and climatic influences on mountain biodiversity. *Nat. Geosci.* **11**, 718–725 (2018).

16. Wiens, J. J. & Graham, C. H. Niche conservatism: integrating evolution, ecology, and conservation biology. *Annu. Rev. Ecol. Evol. Syst.* **36**, 519–539 (2005).

17. Graham, C. H. & Fine, P. V. A. Phylogenetic beta diversity: linking ecological and evolutionary processes across space in time. *Ecol. Lett.* **11**, 1265–1277 (2008).

18. Lozupone, C. & Knight, R. UniFrac: A new phylogenetic method for comparing microbial communities. *Appl. Environ. Microbiol.* **71**, 8228–8235 (2005).

19. Swenson, N. G. Phylogenetic Beta Diversity Metrics, Trait Evolution and Inferring the Functional Beta Diversity of Communities. *PLoS One* **6**, e21264 (2011).

20. Duarte, L. D. S., Bergamin, R. S., Marcilio-Silva, V., Dos Santos Seger, G. D. & Mendes Marques, M. C. Phylobetadiversity among forest types in the Brazilian Atlantic Forest complex. *PLoS One* **9**, e105043 (2014).

21. Wiens, J. J. & Donoghue, M. J. Historical biogeography, ecology and species richness. *Trends Ecol. Evol.* **19**, 639–644 (2004).

22. Crisp, M. D. *et al.* Phylogenetic biome conservatism on a global scale. *Nature* **458**, 754–756 (2009).

23. Holt, B. G. *et al.* An update of Wallace's zoogeographic regions of the world. *Science.* **339**, 74–78 (2013).

24. Jetz, W., Thomas, G. H., Joy, J. B., Hartmann, K. & Mooers, A. O. The global diversity of birds in space and time. *Nature* **491**, 444–448 (2012).

25. Bacon, C. D. *et al.* Biological evidence supports an early and complex emergence of the Isthmus of Panama. *Proc. Natl. Acad. Sci.* **112**, 6110–6115 (2015).

26. Gaston, K. J. *et al.* Spatial turnover in the global avifauna. *Proc. R. Soc. B Biol. Sci.* **274**, 1567–1574 (2007).

27. Barnagaud, J. Y. *et al.* Biogeographical, environmental and anthropogenic determinants of global patterns in bird taxonomic and trait turnover. *Glob. Ecol. Biogeogr.* **26**, 1190–1200 (2017).

28. Schluter, D. & Pennell, M. W. Speciation gradients and the distribution of biodiversity. *Nature* **546**, 48–55 (2017).

29. McKenna, D. D. & Farrell, B. D. Tropical forests are both evolutionary cradles and museums of leaf beetle diversity. *Proc. Natl. Acad. Sci.* **103**, 10947–10951 (2006).

30. McFadden, I. R. *et al.* Temperature shapes opposing latitudinal gradients of plant taxonomic and phylogenetic β diversity. *Ecol. Lett.* **22**, 1126–1135 (2019).

31. Stebbins, G. L. *Flowering plants: evolution above the species level*. (1974).

32. Materials and methods are available as supplementary materials at the Science website.

33. Myers, N., Mittermeier, R. A., Mittermeier, C. G., Da Fonseca, G. A. B. & Kent, J. Biodiversity hotspots for conservation priorities. *Nature* **403**, 853–858 (2000).

34. Graham, C. H. *et al.* The origin and maintenance of montane diversity: integrating evolutionary and ecological processes. *Ecography.* **37**, 711–719 (2014).

35. Donoghue, M. J. A phylogenetic perspective on the distribution of plant diversity. *Proc. Natl. Acad. Sci.* **105**, 11549–11555 (2008).

36. Staver, A. C., Archibald, S. & Levin, S. A. The global extent and determinants of savanna and forest as alternative biome states. *Science.* **334**, 230–232 (2011).

37. Koleff, P., Lennon, J. J. & Gaston, K. J. Are there latitudinal gradients in species turnover? *Glob. Ecol. Biogeogr.* **12**, 483–498 (2003).

38. Kraft, N. J. B. *et al.* Disentangling the drivers of beta diversity along latitudinal and elevational gradients. *Science.* **333**, 1755–1758 (2011).

ACKNOWLEDGMENTS

We thank members of the CG, NZ and LP research groups and Jasmine Rajbhandary for comments, and Julie Marin for assistance with data formatting. IM, RW and CG were supported by the European Research Council (ERC) under the European Union Horizon 2020 research and innovation program (No. 787638 granted to CG) and the Swiss National Science Foundation (No. 173342 granted to CG). TR and FC were supported by a visiting fellowship from the Swiss Federal Research Institute WSL, as well as CAPES and INCT-EECBio grants (No. 465610) from the government of Brazil. IM, CG, NZ, and LP consider this publication a contribution to the WSL Lighthouse in Biodiversity Initiative.

AUTHOR CONTRIBUTIONS

IM and TR conceived the partition method with input from RW, CG and MC. IM performed the analyses and wrote the first draft with CG and all authors contributed substantially to revisions.

COMPETING INTERESTS

The authors declare no competing interests.

MATERIALS & CORRESPONDENCE

Correspondence and requests for materials should be addressed to Ian R. McFadden, ian.mcfadden@wsl.ch, Swiss Federal Research Institute WSL, Zürcherstrasse 111, 8903 Birmensdorf, Switzerland

METHODS

Partitioning turnover into recent and ancestral components

To infer the relative importance of more modern and deep-time processes shaping assemblages, we developed a method which partitions phylogenetic turnover into recent and ancestral components. Our method is a significant advance over existing phylogenetic β diversity metrics, as single metrics tend to emphasize either recent or deep-time turnover[19], making comparisons between metrics difficult. It is also an advance compared to phylogenetic tree scaling methods via delta transformations[39], that are now being used in β diversity studies[40,41]. This is because existing methods weight either recent or ancestral sections of the tree when calculating turnover, without completely removing the influence of one time period when quantifying turnover in the other. Our method can be applied to any β diversity metric that uses branch lengths, however for this study we chose to partition a widely-used phylogenetic analog of Jaccard dissimilarity, the UniFrac metric[18]:

$$p\beta_{UniFrac} = \frac{B + C}{A + B + C} \quad (1),$$

where given two assemblages j and k, the sum of branch lengths shared between j and k is given by A, the sum of branch lengths found in assemblage j but not in assemblage k is denoted with B, and the sum of branch lengths found in assemblage k but not in assemblage j is denoted with C. Summing B with C and dividing by the total branch length or phylogenetic diversity (PD_{total}, or $A + B + C$) yields the non-shared, or unique, fraction of branch length (Fig. 1A). As with Jaccard dissimilarity, larger fractions indicate higher turnover between two assemblages.

To create the two additive recent and ancestral turnover partitions we apply a threshold at phylogenetic depth T (units: myr) to the total phylogeny of both assemblages, dividing the tree into two parts (Fig. 1B&C). The ancestral segment of the phylogeny is made by collapsing all branch lengths younger, i.e. closer to the tips, than T to zero, and this truncated tree is then used to calculate the same quantities B and C as above using only the ancestral phylogeny:

$$p\beta_{\text{Ancestral}} = \frac{B_A^T + C_A^T}{A + B + C} \quad (2),$$

where B_A^T is the sum of branch lengths in the ancestral phylogeny made with threshold T that are found in assemblage j but not in assemblage k, and C_A^T is the sum of branch lengths in the ancestral phylogeny made with threshold T found in assemblage k but not in assemblage j. All other quantities are the same. Then, as for UniFrac, the non-shared branch length in the ancestral phylogeny is divided by the total branch length to yield the ancestral turnover fraction. Next, the recent phylogeny is produced by collapsing all branch lengths older, i.e. closer to the root, than T to zero and the quantities B and C are calculated:

$$p\beta_{\text{Recent}} = \frac{B_R^T + C_R^T}{A + B + C} \quad (3),$$

where B_R^T is the sum of branch lengths in the recent phylogeny made with threshold T that are found in assemblage j but not in assemblage k, and C_R^T is the sum of branch lengths in the recent phylogeny made with threshold T found in assemblage k but not in assemblage j. Finally, the quantities are used to calculate recent turnover in the same way as is done for ancestral turnover. Importantly, the turnover values of the two partitions sum to total turnover as obtained with the UniFrac metric:

$$p\beta_{Total} = p\beta_{Ancestral} + p\beta_{Recent} \quad (4).$$

Finally, to remove assemblages without sufficient phylogenetic history to partition, we set a minimum tree depth, or oldest node, of 10myr for the combined phylogeny of both assemblages in each pairwise comparison.

Distribution data

We obtained range polygons for a total of 9,655 bird species from the BirdLife International database[42], which represents the current best estimate of global distributions from a consensus of many sources. Unlike previous studies (*e.g.* Barnagaud *et al.* 2017), we chose to retain widespread and transient species such as shorebirds and birds of prey because our goal was to quantify the total assemblage turnover of all species in all regions. To determine the composition of each local assemblage we aggregated range polygons into 1-degree cells by finding all species with ranges overlapping that cell. Cells with fewer than seven adjacent neighbors were removed to ensure a similar area was compared for each turnover calculation. This resulted in the removal of small islands and areas at the margins of continents, and a total of 12,499 remaining cells.

Phylogenetic relationships

We used the Time Tree of Life database[43] to obtain a complete phylogenetic hypothesis for all bird species. The phylogeny was constructed by mapping many individual molecular phylogenies and divergence data onto a backbone tree based on community consensus; see Hedges *et al.* (2015) for additional information about construction methods. Of the 9,655 bird species with mapped ranges, 86% had phylogenetic information, which yielded a total of 8,296 focal species. For each assemblage (1-degree cell) we calculated phylogenetic diversity as the

356 total branch length connecting all species in the phylogeny[44] and tree depth as the age of the
357 oldest node in the phylogeny. We then created an integrated variable describing the evolutionary
358 structure, or tree topology, of each assemblage using the first axis of a principal component
359 analysis (PCA) combining richness, phylogenetic diversity and tree depth (Extended Data Fig.
360 2B), which explained 78% of the total variation. This allowed us to assess the influence of
361 regional species diversity and phylogenetic topology on turnover fractions[38,45].
362
363 **Climatic and topographic data**
364 To quantify the influence of climate and earth surface topography on turnover partitions, we
365 compiled climatic data from the CHELSA database[46] and topographic data from the EarthEnv
366 database[47], which is derived largely from the USGS Global Multi-resolution Terrain Elevation
367 Data source[48]. We focused on six key topo-climatic attributes, namely mean annual temperature
368 and temperature seasonality, annual precipitation and precipitation seasonality, and finally
369 elevation and total elevational range. To match the geographic scale at which turnover is
370 calculated (see 'Mapping turnover hotspots' below), attribute values for each cell were
371 calculated as the average of the focal cell and all 7-8 neighboring cells. We then used PCA to
372 create two major axes of climatic and topographic variation (Extended Data Fig. 2A) for use in
373 further analyses, which together explained 65.7% of the total variation.
374
375 **Mapping turnover hotspots**
376 We mapped turnover components in space by first calculating total, recent and ancestral turnover
377 between each focal cell and the 7-8 neighboring cells around it, i.e. the Queens's case. Then, the
378 7-8 pairwise turnover calculations were averaged into a single value for each cell (Extended Data

Fig. 3). Next, in order to map the hotspots, we identified cells with turnover in the 90th percentile globally for ancestral and recent turnover separately, and designated these high turnover areas as hotspots of ancestral or recent turnover, respectively. We then overlaid these two sets of focal cells to create the global turnover hotspot map (Fig. 2A) which includes four categories: i) ancestral turnover hotspots, ii) recent turnover hotspots, iii) hotspots of both ancestral and recent turnover and iv) non-hotspot regions with turnover in the 0-90th percentile for both recent and ancestral partitions. Finally, we plotted turnover hotspots in bivariate space using the climatic and topographic PC axis scores for each cell (Fig. 2C).

Modeling drivers of turnover

To test our hypotheses about how recent and ancestral turnover may influence bird richness globally, we modeled richness as a function of each turnover component separately (Fig. 2B). Richness was log-transformed and ancestral and recent turnover were logit-transformed prior to analysis. Due to non-linearity of the relationships a third-degree polynomial fit was used. In addition, we implemented a multivariate modeling framework to understand the relative importance of climate, tree topology, and earth surface topography for predicting phylogenetic turnover, and its recent and ancestral components. To do this we used the total, ancestral and recent turnover values of each cell as the response, and the corresponding PC axis values of climate, topography (see 'Climatic and topographic data' and Extended Data Fig. 2) and tree topology (see 'Phylogenetic relationships' above) as predictors. To quantify the relative importance of each predictor in explaining the total variance of each model we used the lmg method of hierarchical partitioning[49], as implemented in the 'relaimpo' R package[50].

Controlling for richness

The extent to which turnover is influenced by richness is a subject of ongoing debate[38,51]. However, it is thought that metrics comparing a single pair of assemblages, such as Jaccard dissimilarity or UniFrac, are less influenced by richness than so-called 'classical' metrics which include regional or ɣ diversity in the calculation[51]. Nevertheless, to examine any influence of variation in species richness on our results, we mapped in space the residuals from a regression of both ancestral and recent turnover against the richness of each 1-degree cell (Extended Data Fig. 6), logit-transforming both turnover components and log-transforming richness values prior to fitting the model. If geographic variation in turnover was due mostly or entirely to variation in species richness, we would expect no consistent spatial patterning in the residuals, however this was not the case and strong patterns were observed.

Influence of species-poor regions

To further explore the effect of species richness on the spatial distribution of turnover hotspots (see also 'Controlling for richness' above), we systematically removed the most species-poor cells and used the remaining cells to recalculate and remap hotspots of turnover for three lower bound values (Extended Data Fig. 7). We first removed cells in the bottom 10th percentile by richness, next the bottom 25th and finally the bottom 50th percentile- i.e. cells containing less than 21, 76 and 129 species, respectively. If species-poor cells do not influence the size and location of the turnover hotspots, we would expect little or no change in the configuration of hotspot regions as species-poor cells are removed, such as those in the bottom 10th percentile. However, it is expected that some changes will occur in the configuration of hotspots once larger numbers of cells are removed, such as all those below the 25th and 50th percentiles.

Effect of varying threshold depth

To test for an effect of the phylogenetic age at which the tree is divided into recent and ancestral portions, i.e. the chosen threshold depth T, we recalculated ancestral and recent turnover for each cell using two additional threshold values (Extended Data Fig. 1). First, we used a more inclusive threshold of 10myr to define the recent partition (0-10myr), as compared to the 5myr threshold used in the main analyses. Second, we used a less inclusive threshold of 0.5myr, in which branch length from 0-0.5myr was considered recent turnover. If choice of threshold depth has a strong influence on the results, we would expect to see different spatial patterns of turnover among the three threshold values. However, the patterns were nearly identical except that the maximum value of recent turnover decreased, and ancestral turnover increased, as the threshold approached zero (i.e. modern day, Extended Data Fig. 1). All analyses were performed in R 4.0.1[52].

Data availability

Bird range and phylogenetic data used in this study are available from the BirdLife International (http://datazone.birdlife.org/species/requestdis) and TimeTree (http://www.timetree.org) databases, while climatic and topographic data are available from the CHELSA (https://chelsa-climate.org) and EarthEnv databases (http://www.earthenv.org/topography).

Code availability

Code used to calculate recent and ancestral turnover will be archived in a Dryad digital repository (datadryad.org) under a CC0 1.0 Universal Public Domain Dedication license, and is available to editors and referees on request, as is all code used to generate the results.

39. Pagel, M. Inferring the historical patterns of biological evolution. *Nature* **401**, 877–884 (1999).

40. Chalmandrier, L., Münkemüller, T., Lavergne, S. & Thuiller, W. Effects of species' similarity and dominance on the functional and phylogenetic structure of a plant meta-community. *Ecology* **96**, 143–153 (2015).

41. Saladin, B. *et al.* Environment and evolutionary history shape phylogenetic turnover in European tetrapods. *Nat. Commun.* **10**, 1–9 (2019).

42. BirdLife International and NatureServe. Bird Species Distribution Maps of the World. http://datazone.birdlife.org/species/requestdis (2012).

43. Hedges, S. B., Marin, J., Suleski, M., Paymer, M. & Kumar, S. Tree of life reveals clock-like speciation and diversification. *Mol. Biol. Evol.* **32**, 835–845 (2015).

44. Faith, D. P. Conservation evaluation and phylogenetic diversity. *Biol. Conserv.* **61**, 1–10 (1992).

45. Leprieur, F. *et al.* Quantifying phylogenetic beta diversity: distinguishing between 'true' turnover of lineages and phylogenetic diversity gradients. *PLoS One* **7**, e42760 (2012).

46. Karger, D. N. *et al.* Climatologies at high resolution for the earth's land surface areas. *Sci. Data* **4**, 170122 (2017).

47. Amatulli, G. *et al.* A suite of global, cross-scale topographic variables for environmental and biodiversity modeling. *Sci. Data* **5**, 180040 (2018).

48. Danielson, J. J. & Gesch, D. B. *Global Multi-Resolution Terrain Elevation Data 2010 (GMTED2010)*. US Department of the Interior, US Geological Survey (2011).

469 49. Chevan, A. & Sutherland, M. Hierarchical partitioning. *Am. Stat.* **45**, 90–96 (1991).

470 50. Grömping, U. Relative importance for linear regression in R: The package relaimpo. *J.*
471 *Stat. Softw.* **17**, 1–27 (2006).

472 51. Bennett, J. R. & Gilbert, B. Contrasting beta diversity among regions: how do classical
473 and multivariate approaches compare? *Glob. Ecol. Biogeogr.* **25**, 368–377 (2016).

474 52. R Core Team. R: A language and environment for statistical computing. (2013).

EXTENDED DATA

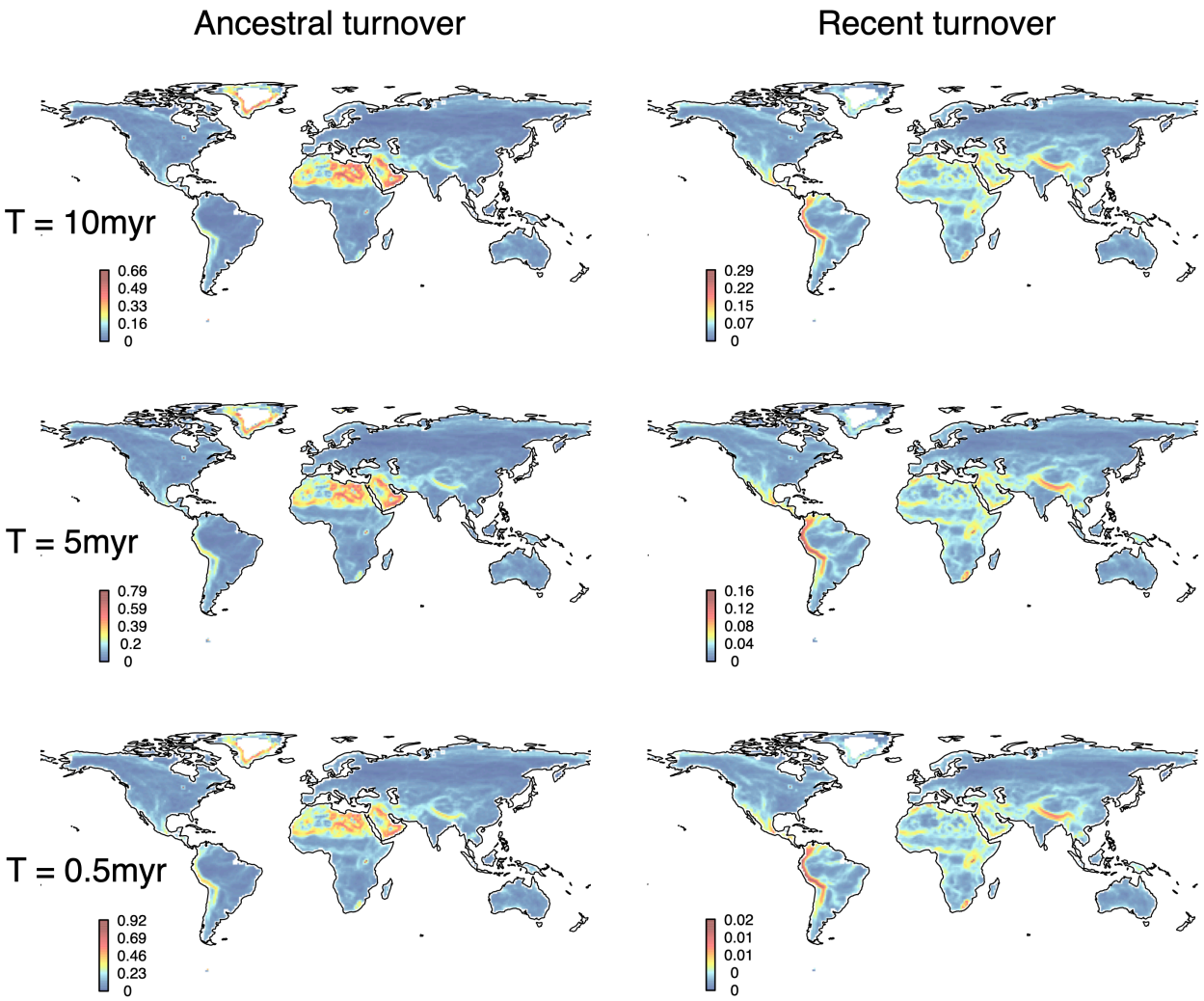

Extended Data Figure 1 | Effect of threshold depth on turnover partitions. Ancestral and recent turnover recalculated using a more temporally inclusive threshold (T) of 10myr to define the recent partition, and a less-inclusive threshold of 0.5myr. Note spatial patterns of turnover remain largely the same for both partitions at all values of the threshold. However, as T approaches zero from the top row to the bottom row, the maximum value of ancestral turnover ($p\beta_{Ancestral}$) increases and the maximum value of recent turnover ($p\beta_{Recent}$) decreases.

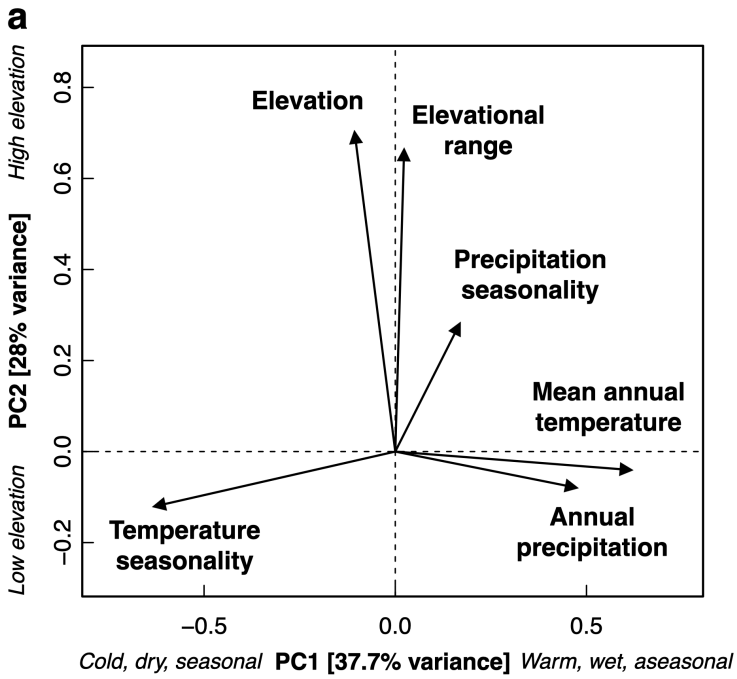

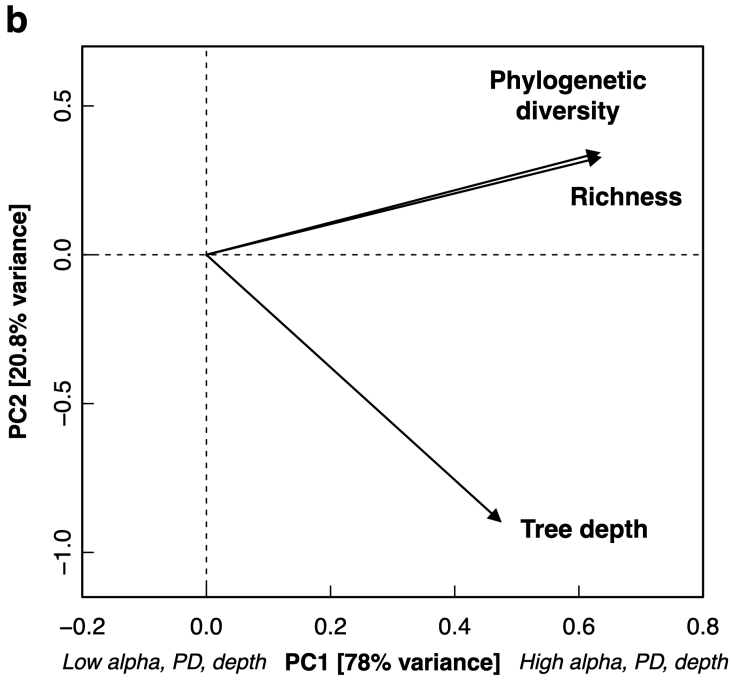

Extended Data Figure 2 | Major axes of variation in climate, topography and tree topology. (**a**) Principal component axes representing macroclimatic (PC1) and topographic variation (PC2). (**b**) Tree topology measure (PC1), calculated for each 1-degree cell. The measure integrates species richness (alpha), phylogenetic diversity (PD)- total branch length connecting all species- and tree depth, the total divergence time between root and tip of an assemblage phylogeny.

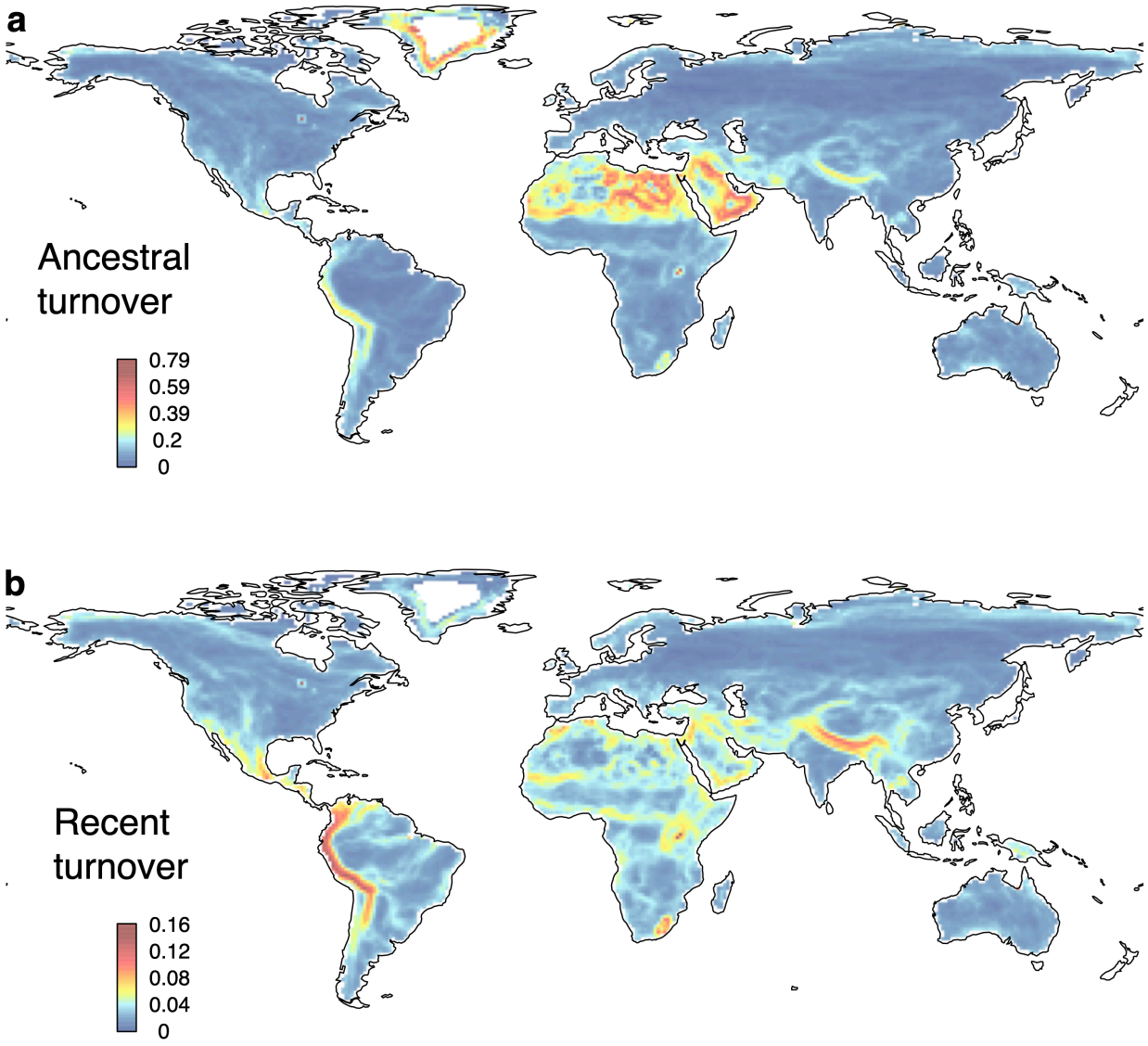

Extended Data Figure 3 | Maps of continuous ancestral and recent turnover. Maps of single turnover partitions used to define the global turnover hotspots using a threshold of 5myr. Note the smaller maximum value of recent ($p\beta_{Recent}$) compared to ancestral ($p\beta_{Ancestral}$) turnover.

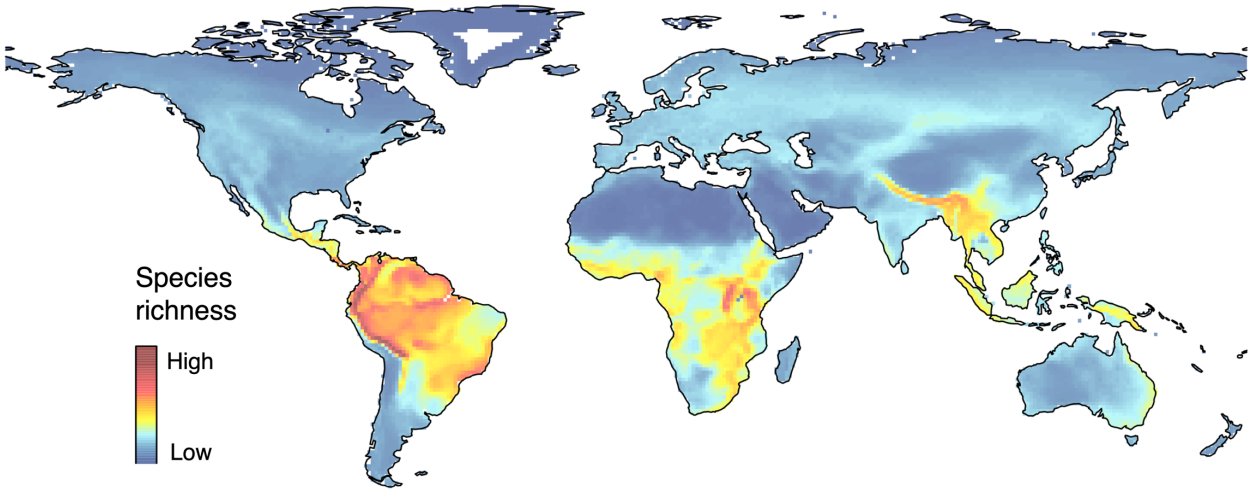

Extended Data Figure 4 | Global bird richness patterns. Richness values were calculated by aggregating range maps into 1-degree cells. Note the high richness of tropical and subtropical mountainous regions, as well as Amazonian lowlands.

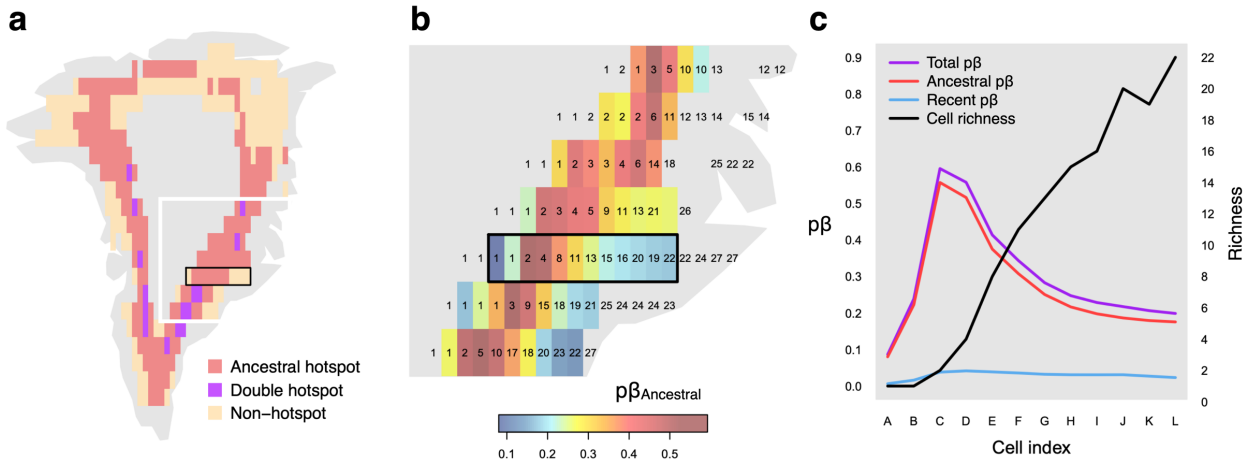

Extended Data Figure 5 | Influence of species-poor assemblages on ancestral turnover. As shown here for Greenland, several regions of high ancestral turnover ($p\beta_{Ancestral}$) are species-poor and adjacent to areas of higher richness. (**a**) Greenland map with colors corresponding to turnover hotspots. White inset shows the focal area (**b**) containing a horizontal grid cell transect (black rectangle), for which the total, ancestral and recent turnover ($p\beta$), and richness of the 12 cells is plotted left to right along the transect (**c**). (**b**) Colors within each cell are ancestral turnover values and numbers within cells indicate richness.

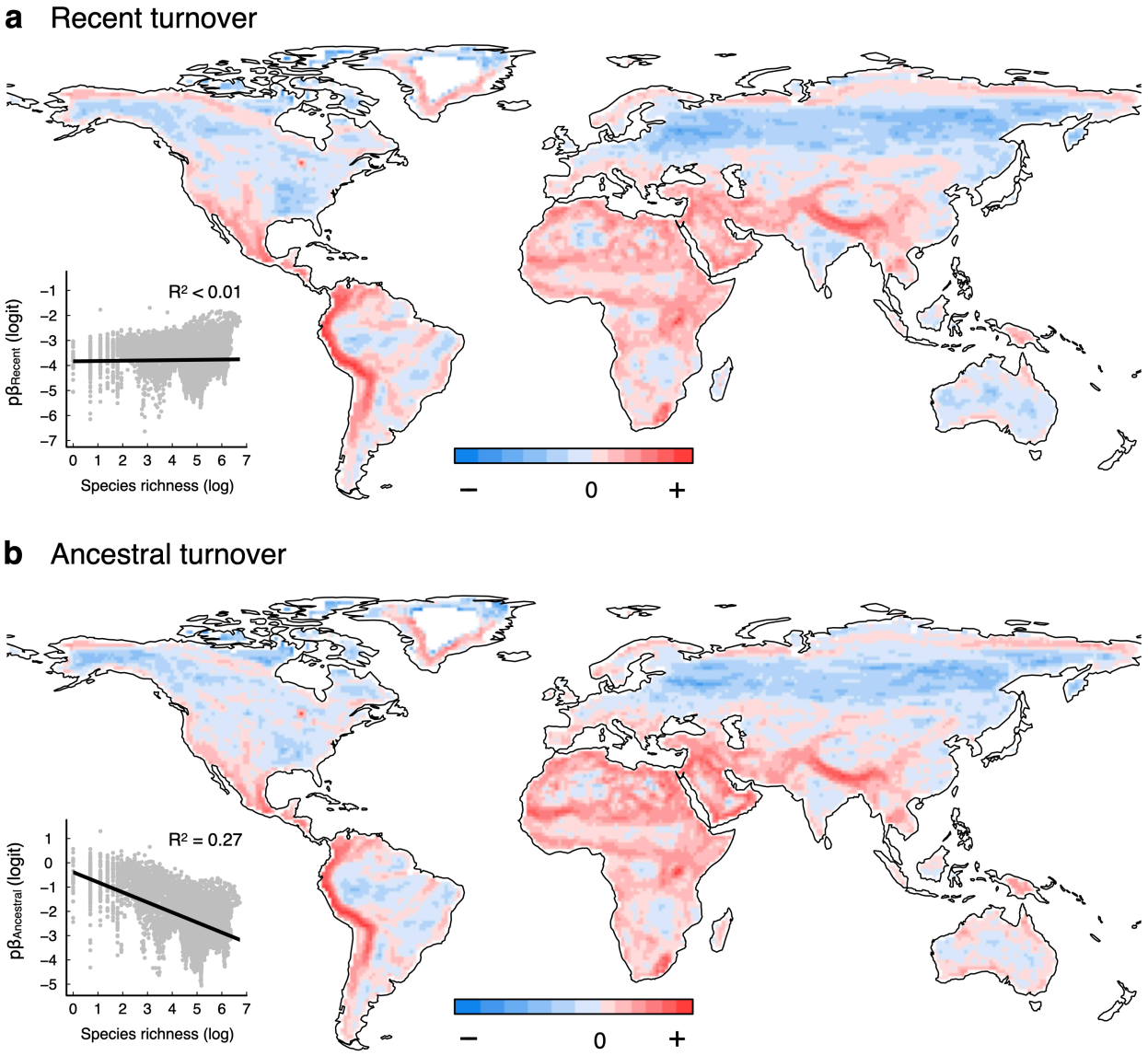

Extended Data Figure 6 | Effect of local richness on turnover partitions. Residuals of regressions between turnover components and richness (insets) for each 1-degree cell plotted in geographic space. Colors correspond to positive (red) and negative (blue) residual values. Note strong geographic structure in residuals for both components.

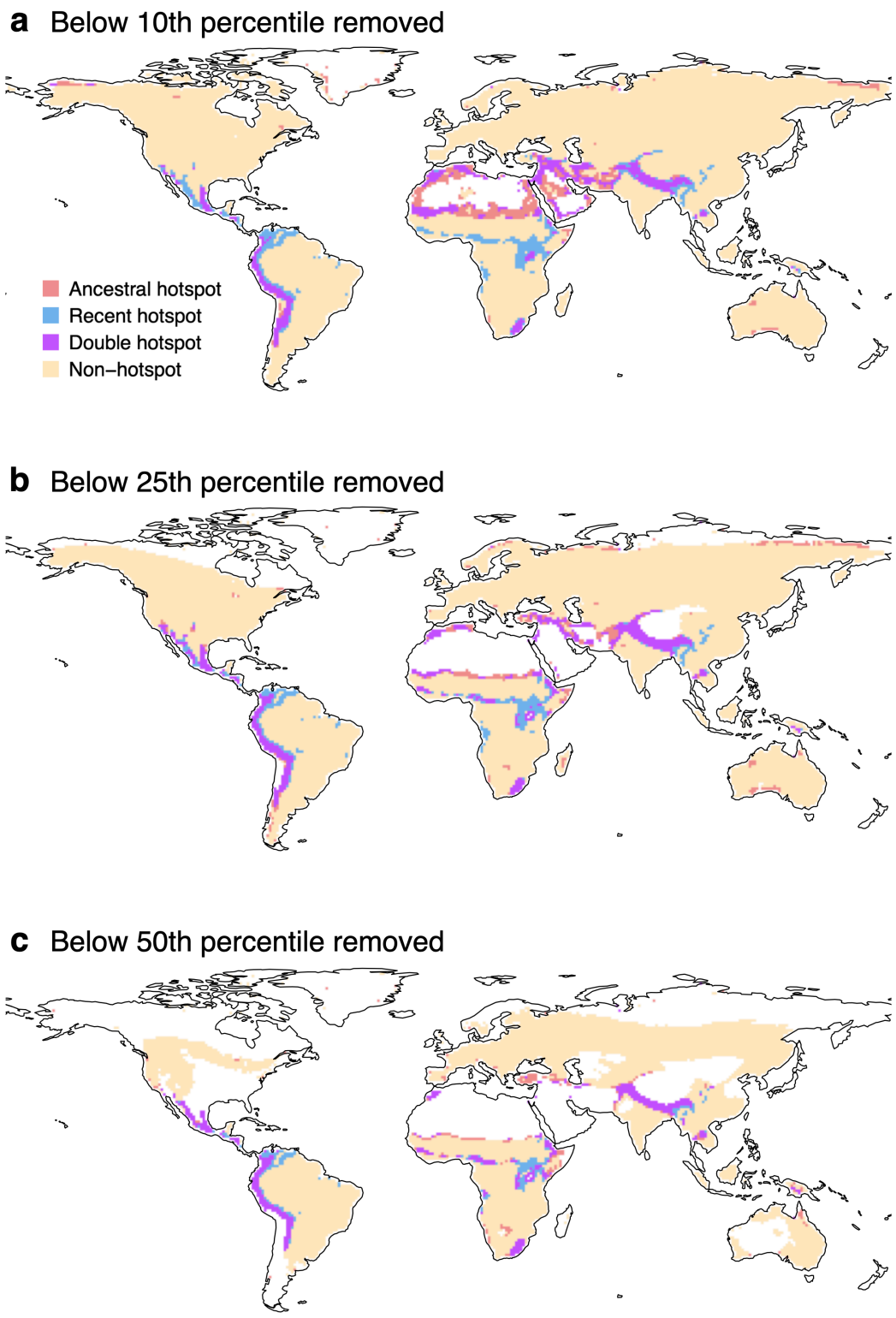

503 **Extended Data Figure 7 | Effect of removing low diversity cells on turnover hotspots.** Cells
504 below a given percentile (10th, 25th, and 50th) were removed, and recent ($p\beta_{Recent}$) and ancestral
505 ($p\beta_{Ancestral}$) hotspots were recalculated and plotted as in the main text (**a**-**c**).